analytical chemistry

Article

pubs.acs.org/ac

Facile Synthesis of Boronate-Decorated Polyethyleneimine-Grafted Hybrid Magnetic Nanoparticles for the Highly Selective Enrichment of Modified Nucleosides and Ribosylated Metabolites

Hua Li, Yuanhong Shan, Lizhen Qiao, Abo Dou, Xianzhe Shi,* and Guowang Xu*

CAS Key Lab of Separation Sciences for Analytical Chemistry, Dalian Institute of Chemical Physics, Chinese Academy of Sciences, Dalian 116023, China

Supporting Information

ABSTRACT: Ribosylated metabolites, especially modified nucleosides, have been extensively evaluated as cancer-related biomarkers. Boronate adsorbents are considered to be promising materials for extracting them from complex matrices. However, the enrichment of ribosylated metabolites in low abundance is still a challenge due to the limited capacity and selectivity of the existing boronate adsorbents. In this study, a novel type of magnetic nanoparticles named Fe_3O_4@SiO_2@PEI-FPBA was synthesized by grafting polyethyleneimine (PEI) onto the surface of Fe_3O_4@SiO_2 before modification by boronate groups. The high density of the amino groups on the PEI chains supplied a large number of binding sites for boronate groups. Thus, the adsorption capacity (1.34 ± 0.024 mg/g) of the nanoparticles, which is 6- to 7-fold higher than that of analogous materials, was greatly improved. The unreacted secondary amines and tertiary amines of the PEI enhanced the aqueous solubility of the nanoparticles, which could efficiently reduce nonspecific adsorption. The nanoparticles were able to capture 1,2 cis-diol nucleosides from 1000-fold interferences. Moreover, the flexible chains of PEI were favorable for effective enrichment and quick equilibration (<2 min). Finally, 60 ribose conjugates were enriched from human urine using the nanoparticles. Among them, 43 were identified to be nucleosides and other ribosylated metabolites. Nine low abundance modified nucleosides were detected for the first time. In conclusion, Fe_3O_4@SiO_2@PEI-FPBA is an attractive candidate material for the highly selective enrichment of 1,2-cis-diol compounds.

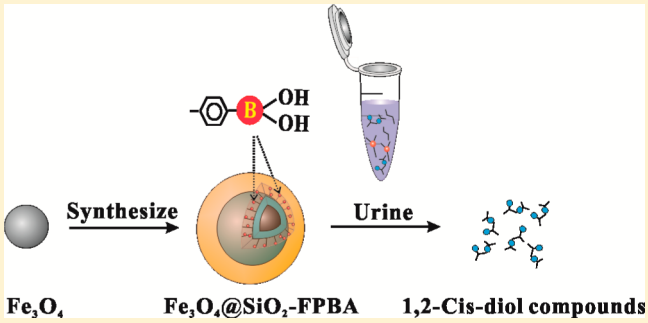

Ribonucleic acids (RNA) play crucial roles in many fundamental bioprocesses, and modifications in their bases or ribose are closely correlated with bioactivity.[1] Ribonucleosides as end products directly reflect the degradation rate of the RNA. Due to the lack of phosphorylases in cells, modified nucleosides cannot be reused as normal nucleosides for RNA synthesis and are thus excreted from the cell into the biofluids.[2] In tumor cells, the impaired tRNA metabolism usually leads to abnormal levels of modified nucleosides.[3] Therefore, modified nucleosides have been extensively studied in the search for cancer-related biomarkers.[4−6]

Previous research has focused mainly on the detection of several common modified nucleosides in urine through chromatography or capillary electrophoresis coupled with mass spectrometry (MS) or UV detection.[7−11] Detection of potentially unknown modified nucleosides is significant for discovering new cancer biomarkers. However, the low concentrations and serious matrix interferences in the biological samples set great obstacles for their detection. Therefore, appropriate pretreatment approaches are necessary for the comprehensive analysis of nucleosides.

Online solid phase extraction (SPE) purification by aprotic boronic acid chromatography (ApBAC) encounters an incompatibility issue between the loading solvents and the separation solvents.[12,13] For offline purification, commercial SPE columns, including Oasis WCX, Bond Elut Plexa, and Oasis HLB, based on the ion exchange or mixed mode present poor specificity and low absolute recovery.[14−16] Boronate affinity adsorbents such as Affi-Gel 601 have been widely applied as promising materials for the specific capture of nucleosides because boronic acid groups can reversibly form five- or six-membered cyclic esters with cis-diol compounds when the pH of the solution is altered.[17] However, laborious manipulation and low loading capacity are significant limitations of these materials.[18−20] Recently, boronate-functionalized nanoadsorbents have attracted wide attention,[21−23] especially magnetic nanoparticles,[24−26] for their large surface-to-area ratio, quick magnetic resonance, and controllable surface modification. Although a simplified pretreatment process has been realized, the adsorption capacity and selectivity are not satisfactory for biological sample analysis. To improve the adsorption capacity, mesoporous structures

Received: September 18, 2013
Accepted: October 30, 2013
Published: October 30, 2013

were generally formed on the surface of the magnetic nanoparticles or long chain polymers were grafted by atomic transfer radical polymerization (ATRP).[27,28] Unfortunately, the mesoporous structures usually restricted internal mass transport, and the ATRP reaction must be carried out under strictly anaerobic conditions.[28,29] To improve the selectivity, an extra modification with biocompatible poly(ethylene glycol) was often used to reduce nonspecific adsorption. However, multistep complicated chemical modifications increased the preparation difficulty of the magnetic nanoparticles.[28]

In this study, a novel magnetic nanoparticle named Fe_3O_4@SiO_2@PEI-FPBA with large adsorption capacity and high selectivity was synthesized by a facile approach. The long-chain polyethyleneimine (PEI) with a high density of amino groups was first grafted onto the surface of Fe_3O_4@SiO_2 by reductive amination. The amino groups of PEI not only could provide enormous reaction sites for boronate binding but also could improve the hydrophilicity of the nanoparticles to reduce the nonspecific adsorption. The selectivity and adsorption capacity of the novel material were evaluated using 1,2-cis-diol nucleosides with noncis-diol or 1,3-cis-diol analogues used as interfering compounds. Finally, Fe_3O_4@SiO_2@PEI-FPBA was applied to extract nucleosides and ribosylated metabolites from urine. These ribose conjugates were identified by in-house developed neutral loss software, along with accurate molecular mass obtained from MS.

EXPERIMENTAL SECTION

Materials. Ferric acetylacetonate was purchased from Aladdin (Shanghai, China). Igepal CO-520, ammonium acetate (NH_4AC), formic acid (FA), tetraethoxysilane (TEOS), aminopropyltriethoxysilane (APTES), ammonium hydroxide (28−30%), and all of the nucleoside standards were obtained from Sigma (St. Louis, MO). Glacial acetic acid was obtained from Tedia (Fairfield, OH). Ethanol, *n*-octanol, *n*-octylamine, pentanedial, and cyclohexane were all analytical grade reagents. Boronate affinity gel (BAG) was obtained from Biorad (Munich, Germany). Isopropanol, methanol, and acetonitrile were obtained from Merck (Dermstadt, Germany). Water was purified by a Milli-Q system (Millipore, Milford, MA). PEI [M_w = 10000 (10T) and 750000 (750T)] and 4-formylphenylboronic acid (4-FPBA) were purchased from Alfa Aesar (Tianjin, China).

Synthesis of Fe_3O_4@SiO_2@PEI-FPBA. Fe_3O_4 magnetic nanoparticles were synthesized through a hydrothermal method, as described in the literature.[30] After being washed several times with cyclohexane, Fe_3O_4 was dispersed into cyclohexane. For encapsulating the Fe_3O_4 into silica (denoted as Fe_3O_4@SiO_2), a W/O microemulsion technique was used, as reported in the literature.[31] After the generated Fe_3O_4@SiO_2 nanoparticles were rinsed with ethanol and isopropanol, 1 g of Fe_3O_4@SiO_2 was dispersed into 600 mL of isopropanol. Sequentially, 10 mL of APTES was added dropwise to the mixture while it was mechanically stirred for 24 h at room temperature under argon protection. The functionalized Fe_3O_4@SiO_2 nanoparticles with amino groups (denoted as Fe_3O_4@SiO_2−NH_2) were isolated and washed several times with methanol. After the dispersion of the Fe_3O_4@SiO_2−NH_2 into 300 mL of acetic acid/methanol (v/v, 1:125, mixed solvent *i*), 3 mL of pentanedial was added, and the reaction was allowed to continue for 10 h at 40 °C to generate the Schiff base. The resulting products (denoted as Fe_3O_4@SiO_2−CHO) were collected and washed with the mixed solvent *i* to remove excess pentanedial and then were redispersed into 300 mL of mixed solvent *i* again. Similarly, PEI and 4-FPBA were grafted step-by-step onto the surface of Fe_3O_4@SiO_2−CHO through the reaction between the aldehyde and amino groups, and 300 mg of $NaBH_3CN$ was added to reduce the unstable Schiff base. Finally, the obtained Fe_3O_4@SiO_2@PEI-FPBA nanoparticles were washed several times with ethanol and water.

Characterization. The size, morphology, and dispersion of the nanoparticles were observed with transmission electron microscopy (TEM) (JEM-2000EX, JEOL, Japan). Fourier-transform infrared spectra (FT-IR) (EQUINOX 55, BRUKER, Germany) was used to record the group changes on the surfaces of the nanoparticles. Magnetization curves of Fe_3O_4@SiO_2@PEI-FPBA nanoparticles were measured by a vibrating sample magnetometer (JDM-13, Jilin University, China). X-ray photoelectron spectroscopy (XPS) (ESCALAB250Xi, Thermo Scientific) determined the surface compositions of the materials. Zeta-potential (Zetasizer Nano, Malvern, United Kingdom) was used to show the surface conversion of the Fe_3O_4@SiO_2 after the binding of the amino groups. An inductively coupled plasma-optical emission spectrometer (ICP-OES) (Optima2000DV, PerkinElmer) was used for the quantitative detection of boron in Fe_3O_4@SiO_2@PEI-FPBA.

Optimization of the Extraction and Desorption Conditions. The pH and equilibration time of both the extraction and desorption were investigated, respectively. An adenosine (A) solution at a concentration of 20 μg/mL was chosen as the test solution. When optimizing the extraction pH and equilibration time, 1 mL of the A solution was adjusted to different pH values with ammonium hydroxide followed by incubation with Fe_3O_4@SiO_2@PEI(750T)-FPBA nanoparticles. After 30 s sonication dispersion and various time of vortex shaking (from 0.5 min to 2 h), the magnetic nanoparticles were isolated with the magnet and the free A in the supernatant was detected via ultraviolet detection at 260 nm. When optimizing the pH and equilibration time of desorption, the extraction pH and equilibration time were adopted from the optimized conditions determined above. After incubating the A solution with the nanoparticles, the supernatant was discarded and 1 mL of FA solution at different concentrations was used to elute the adsorbed A from the nanoparticles. The desorption time varied from 0.5 to 30 min, and the eluates were detected by ultraviolet detection at 260 nm.

Selectivity Evaluation of Fe_3O_4@SiO_2@PEI-FPBA. The solution included two 1,2-cis-diol nucleosides, 1-methyladenosine (m_1A), guanosine (G), and two interfering structural analogues, the noncis-diol compounds, 2-deoxyadenosine (DA) and 2′-O-methylguanosine (Gm), at concentrations of 20 nmol/mL, and was used as the model to evaluate the selectivity of the Fe_3O_4@SiO_2@PEI(750T)-FPBA nanoparticles. Of the above solution, 0.1 mL was extracted by the nanoparticles under the optimal conditions. After the supernatant was discarded, the nanoparticles were rinsed three times with 0.2 mL of 0.005% $NH_3{\cdot}H_2O$ (washing solution *i*) and were then eluted with 0.1 mL of 200 mM FA solution (elution solution *i*). To show the purification ability of the nanoparticles from complex samples, 10-fold and 100-fold interferences were added, and the same handling process was repeated. To verify the specific affinity of the nanoparticles toward 1,2-cis-diol compounds, the interferences from the 1,3-cis-diol compounds phenyl-β-D-glucopyranoside (pG) and indican (3-indoxyl-β-D-

dx.doi.org/10.1021/ac402979w | Anal. Chem. 2013, 85, 11585−11592

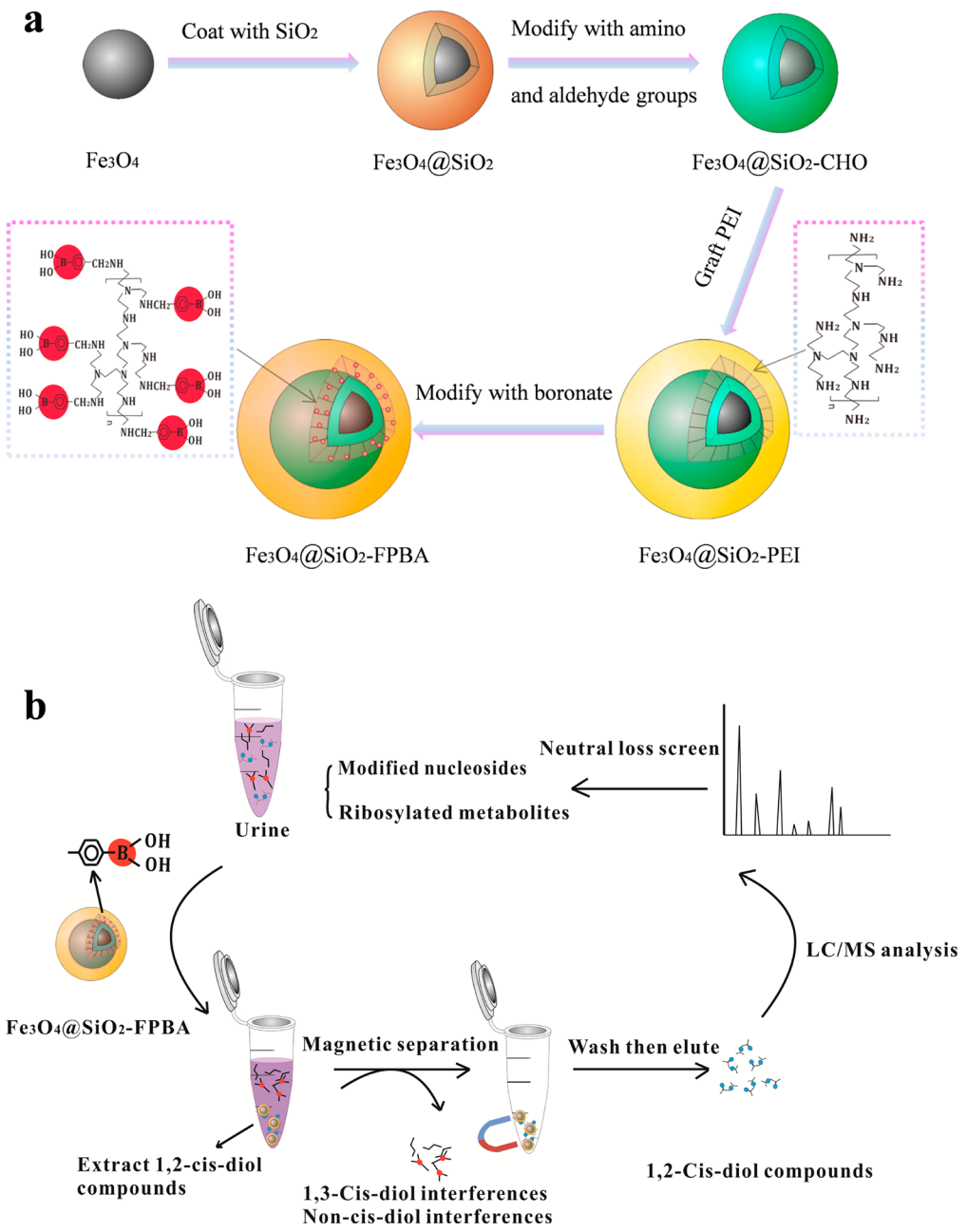

Figure 1. (a) Synthetic strategy for the Fe_3O_4@SiO_2@PEI-FPBA nanoparticles and (b) workflow of the 1,2-cis-diol-containing molecules enrichment from urine using Fe_3O_4@SiO_2@PEI-FPBA nanoparticles.

glucopyranoside) (iiG) with molar ratios of 100:1 and 1000:1 were further evaluated.

Adsorption Capacity Evaluation of Fe_3O_4@SiO_2@PEI-FPBA. Ten milligrams of Fe_3O_4@SiO_2@PEI-FPBA nanoparticles was incubated with 1 mL of the A solution (1 mg/mL) at a pH value of 9 adjusted by $NH_3{\cdot}H_2O$. Sonication and full vortex mixing were applied to reach adsorption equilibration. The materials were isolated and washed several times with washing solution *i* until no A was detected in the supernatant. Finally, 1 mL of elution solution i was used to elute the A.

Commercial BAG was activated with 0.25 M NH_4AC (pH = 8.5), 0.1 M NaCl, and 0.1 M FA in methanol/H_2O (v/v, 1:1),[32] and 10 mg of BAG was used to extract the A that was dissolved in a 0.25 M NH_4AC at a concentration of 1 mg/mL. The following operation was similar as the method used for Fe_3O_4@SiO_2@PEI(750T)-FPBA nanoparticles, except that the washing solution was 0.25 M NH_4AC (washing solution ii), and the elution solution was 0.1 M FA in methanol/H_2O (v/v, 1:1, elution solution ii).

Recovery Evaluation of Fe_3O_4@SiO_2@PEI-FPBA. Twelve nucleoside standards (NSs) were mixed in the following concentrations: 1.28 mM pseudouridine (Pseu), 0.016 mM cytidine (C), 0.032 mM uridine (U), 0.16 mM m_1A, 0.016 mM G, 0.064 mM 1-methylguanosine (m_1G), 0.042 mM N_4-acetylcytidine (ac_4C), 0.032 mM A, 0.016 mM 3-methyluridine (m_3U), 0.016 mM 5′-deoxy-5′-methylthioadenosine (MTA), 0.016 mM inosine (I), and 0.032 mM xanthosine (X). 8-Bromoguanosine (Br_8G) was used at a concentration of 0.3 mM as the internal standard (IS).

After urine was thawed and centrifuged at 15000 rpm for 10 min, 0.2 mL of NSs and 0.1 mL of IS were pooled into 0.5 mL

dx.doi.org/10.1021/ac402979w | *Anal. Chem.* 2013, 85, 11585−11592

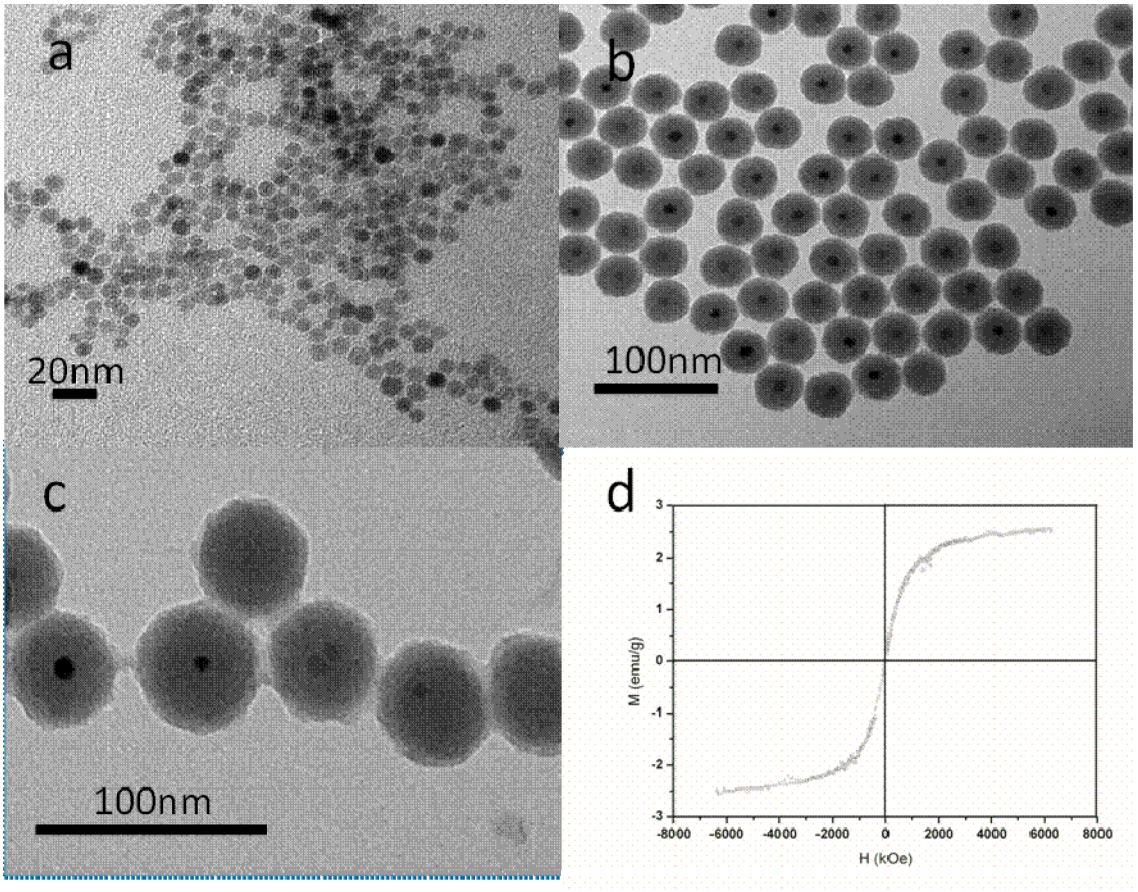

Figure 2. TEM images of (a) Fe_3O_4 nanoparticles, (b) Fe_3O_4@SiO_2 nanoparticles, and (c) Fe_3O_4@SiO_2@PEI(750T)-FPBA nanoparticles. (d) Magnetization curves of the Fe_3O_4@SiO_2@PEI(750T)-FPBA nanoparticles.

of urine, and the mixture was diluted to 1 mL with water. Then, the urine sample was alkalized to a pH of 9 by 0.1% $NH_3 \cdot H_2O$ at a ratio of 19:1 (v/v). Fifteen milligrams of the nanoparticles were incubated with 100 μL of the above pooled urine to extract the nucleosides under the optimal conditions. After rinsing with 200 μL of washing solution i three times to eliminate nonspecific adsorption, 95 μL of elution solution i was added to efficiently elute the analytes. The eluate was analyzed by liquid chromatography–mass spectrometry (LC–MS).

Extraction of the Nucleosides and Ribosylated Metabolites from the Urine. To extract ribose conjugates with Fe_3O_4@SiO_2@PEI(750T)-FPBA nanoparticles, 950 μL of urine was alkalized and then extracted with 150 mg of the magnetic nanoparticles. After rinsing, to eliminate nonspecific adsorption, 1 mL of elution solution i and 1 mL of methanol were used to efficiently elute the analytes. Before extracting the ribose conjugates with 150 mg of BAG, the pH of the urine was adjusted to 8.5. One milliliter of ammonia–water (pH = 8.5) and 0.3 mL of CH_3OH:H_2O (v/v, 1:1) were used to rinse the nanoparticles twice to eliminate nonspecific adsorption, and finally, the trapped ribose conjugates were eluted with 1 mL of elution solution ii. All of the eluates were lyophilized and reconstituted with 40 μL of ACN/H_2O (v/v, 2:98) before LC–MS analysis.

Liquid Chromatography–Mass Spectrometry Analysis. An Agilent 1290 UHPLC system coupled to a triple-quadrupole mass spectrometer (Agilent) with an electrospray ionization (ESI) source in the multi reaction monitor (MRM) mode was used to detect the recoveries of the 12 nucleosides. The parameters of the MRM for NSs and IS are listed in Table S1 of the Supporting Information. A 1 μL urine sample was separated on a BEH C18 column (2.1 × 100 mm, 1.7 μm, Waters, Ireland) at 40 °C with mobile phases A (10 mM ammonium acetate in water) and B (acetonitrile) at an initial gradient of 2% B. The initial ratio was run for 5 min and was then raised to 10% B in 17 min. To rinse the strongly retained components of the urine, the gradient was increased linearly to 100% B within 8 min and maintained for 5 min. An Acquity UPLC system (Waters) coupled to a Triple TOF 5600 (AB SCIEX) with a DuoSpray ion source was used to analyze the extracted urine. The gradient program, analytical column, and column temperature were the same as mentioned above. The injection volume was 5 μL. The mass scan range was set from m/z of 80 to 1000 in the positive mode. The ion spray voltage was kept at 5500 V, and the ion source temperature was set at 500 °C. The ion source gases 1 and 2 and the curtain gas were at pressures of 50, 50, and 35 psi, respectively. The collision energy (CE) was 10 eV, and the declustering potential was maintained at 100 eV.

Data Processing and Database Searching. The raw data of three replicates of each material obtained from the Triple TOF 5600 was processed using MarkerView 1.2.1 for picking up and matching peaks. The parameters used are as follows: minimum retention time, 0.8 min; maximum retention time, 23.6 min; subtraction offset, 30 scans; minimum spectral peak width, 15 ppm; minimum RT peak width, 4 scans; noise threshold, 3; retention time tolerance, 0.15 min; mass tolerance,

dx.doi.org/10.1021/ac402979w | *Anal. Chem.* 2013, 85, 11585–11592

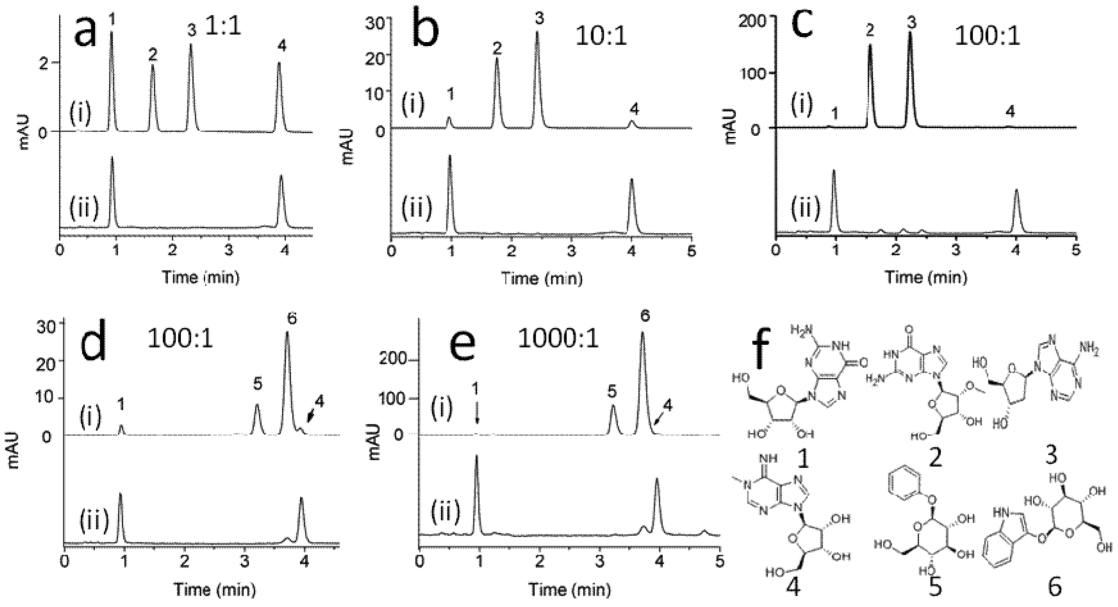

Figure 3. Chromatograms of the mixture of (a–c) noncis-diol-containing molecules or (d and e) 1,3-cis-diol-containing molecules with 1,2-cis-diol-containing molecules analyzed (i) directly and (ii) after enrichment by Fe_3O_4@SiO_2@PEI(750T)-FPBA nanoparticles with molar ratios of 1:1, 10:1, 100:1, 100:1, and 1000:1. (f) Structures of G, Gm, DA, m_1A, pG, and iiG marked as peaks 1–6, respectively.

20 ppm; remove peaks in less than two samples; maximum peaks, 5000. After excluding the isotope peaks, the exported peak table from MarkerView was processed by in-house developed neutral loss software to screen the ion pairs with a m/z difference of 132.0423 ± 0.0026. The drift tolerance of the retention time was less than 0.05 min. Unknown compounds were searched in metlin (http://metlin.scripps.edu/) and the RNA modification database (http://mods.rna.albany.edu/mods/modifications/view/113) for qualification.

RESULTS AND DISCUSSION

Synthesis and Characterization of the Fe_3O_4@SiO_2@PEI-FPBA Nanoparticles. The synthetic procedure for the Fe_3O_4@SiO_2@PEI-FPBA nanoparticles is illustrated in Figure 1a. Briefly, Fe_3O_4 was synthesized by a solvothermal method and was subsequently encapsulated into silica with reverse microemulsion. Then, amino groups were functionalized onto the surface by reacting APTES with silanols on the Fe_3O_4@SiO_2. To expand the number of amino groups further, PEI was grafted onto the surface through a pentanedial linkage by a reductive amination reaction. Finally, 4-FPBA was immobilized onto the nanoparticles. As shown in the TEM image of Figure 2a, Fe_3O_4 nanoparticles show uniformly spherical shapes with diameters of approximately 6–8 nm. After being coated with silica, their size increased to approximately 32 nm in diameter, and good monodispersity was maintained (Figure 2b). The zeta potential of the nanoparticles was changed from −36.9 to 35.3 mV after amino groups were grafted onto their surface, which revealed that a large amount of amino groups were immobilized on the surface of the Fe_3O_4@SiO_2. From the TEM image in Figure 2c, the final Fe_3O_4@SiO_2@PEI-FPBA nanoparticles exhibited a typical sandwich structure. The outer shell with the boronate groups shows a 2–3 nm thickness, and the saturation magnetization of the nanoparticles is 2.52 emu g^{-1}.

From the results of XPS analysis (Table S2 of the Supporting Information), the C and N atomic percentages of Fe_3O_4@SiO_2@PEI(750T) are larger than those of Fe_3O_4@SiO_2–NH_2, which confirmed that PEI was successfully grafted onto the surface of Fe_3O_4@SiO_2–NH_2. The B atom was found in Fe_3O_4@SiO_2@PEI-FPBA, which proved that 4-FPBA was favorably bonded. Moreover, the B atomic percentage of Fe_3O_4@SiO_2@PEI(750T)-FPBA is much higher than that of Fe_3O_4@SiO_2@PEI(10T)-FPBA because the long chain of PEI (750T) can supply more reaction sites to bind 4-FPBA than the short chain of PEI (10T). In addition, Fe is not found in all materials, which denotes that the magnetic cores have been completely encapsulated. FT-IR spectroscopy shown in Figure S1a of the Supporting Information also indicates the successful immobilization of 4-FPBA on the surfaces of the magnetic nanoparticles, as a benzene ring stretching vibration at 1500–1600 cm^{-1}, a B–O stretching vibration at 1355 cm^{-1}, and an O–H bending vibration at 1408 cm^{-1} are obvious. The weight percentage of B in Fe_3O_4@SiO_2@PEI(750T)-FPBA was 0.69% measured quantitatively by ICP-OES. It was calculated to correspond to a high boronate binding amount of approximately 28.4 mg/g, which is 5-fold larger than the previous report.[33]

Evaluation of the Properties of Fe_3O_4@SiO_2@PEI-FPBA Nanoparticles. Boronate groups can form reversible complexes of five- or six-membered cyclic esters with cis-diol-containing molecules under alkaline conditions, and the complexes will be dissociated if the conditions are switched to acidic.[17,34] To realize the best performance of the nanoparticles, the pH values and equilibrium time of the extraction and desorption were optimized individually. The most suitable pH values for extraction and desorption are 9 (0.005% $NH_3 \cdot H_2O$) and 3 (5 mM FA), as shown in Figures S2 and S3 of the Supporting Information. Moreover, the equilibrium of the extraction and desorption were so fast that the whole manipulation could be finished within 2 min (Figures S4 and S5 of the Supporting Information). Compared with SPE materials,[22,32] the manipulation procedures were greatly simplified.

As PEI serves as the linker between 4-FPBA and Fe_3O_4@SiO_2, the chain length of PEI will affect the adsorption capacity of the magnetic materials. Two types of PEI with average

dx.doi.org/10.1021/ac402979w | Anal. Chem. 2013, 85, 11585–11592

Table 1. Ribose Conjugates Enriched from Urine by Fe_3O_4@SiO_2@PEI(750T)-FPBA

no.	t_R (min)	precursor ion	name	error (ppm)
1	0.86	288.1213	*n*-ribosylhistidine	7
2	0.88	255.0979	1-ribosyl-3-carbamoylpyridinium	−1.4
3[ab]	0.97	245.078	pseudouridine	4
4	0.98	247.0922	5,6-dihydrouridine	−1
5[b]	1	244.093	cytidine	0
6	1.15	271.093	clitidine/1-ribosyl-5-carbamoyl-2-oxo-pyridine/1-ribosyl-3-carbamoyl-4-oxo-pyridine	1
7	1.22	258.1076	5-methylcytidine/3-methylcytidine	3
8[c]	1.26	304.1006	5-methylaminomethyl-2-thiouridine	14.4
9[b]	1.29	282.1219	1-methyladenosine	7
10[b]	1.29	285.0815	xanthosine	5
11[b]	1.39	245.0765	uridine	−1
12	1.5	259.1032	1-ribosyl-4-carboxamido-5-aminoimidazole	0.38
13[c]	1.58	301.0779	urate-3-ribonucleoside	0
14[b]	1.66	298.1137	7-methylguanosine	−3
15	1.79	271.0926	clitidine/1-ribosyl-5-carbamoyl-2-oxo-pyridine/1-ribosyl-3-carbamoyl-4-oxo-pyridine	0
16[b]	1.9	284.099	guanosine	0.07
17[b]	2.04	269.0875	inosine	−2
18[c]	2.16	284.0989	isoguanosine	0
19[c]	2.26	333.0932	5-(carboxyhydroxymethyl)uridine methyl ester/uridine 5-oxyacetic acid methyl ester	1.2
20	2.43	271.0929	clitidine/1-ribosyl-5-carbamoyl-2-oxo-pyridine/1-ribosyl-3-carbamoyl-4-oxo-pyridine	1
21[a]	2.98	385.1296	*S*-adenosylhomocysteine	−2
22[c]	3.1	333.0933	5-(carboxyhydroxymethyl)uridine methyl ester/uridine 5-oxyacetic acid methyl ester	1.2
23[b]	3.57	259.0921	3-methyluridine	1
24	3.8	300.1555	1-ribosyl-*N*-*ω*-propionylhistamine	0.66
25	3.88	283.1037	1-methylinosine	0
26[b]	3.93	298.1161	1-methylguanosine	5
27[c]	4.75	317.0973	5-methoxycarbonylmethyluridine	−2.2
28	4.76	298.116	2-methylguanosine	5
29[b]	4.81	286.104	N4-acetylcytidine	2
30[b]	5.24	268.1052	adenosine	4
31	8.01	326.1483	N2 N2 7-trimethylguanosine	7.3
32	8.46	312.1318	dimethylguanosine	4
33	9.84	333.0749	5-methoxycarbonylmethyl-2-thiouridine	−0.6
34	9.91	413.1404	N6-threonylcarbamoyladenosine	−2.9
35	11.26	342.2024	1-ribosyl-N-*ω*-caproyllhistamine	0.21
36[b]	11.58	282.12	6-methyladenosine	7
37[c]	12.59	322.1132	4-demethylwyosine	−4.3
38[c]	12.97	272.1243	N4,N4-dimethylcytidine	0.73
39	13.35	427.1584	N6-methyl-N6-threonylcarbamoyladenosine	2.8
40	14.84	328.1863	1-ribosyl-*N*-*ω*-valerylhistamine	−1.2
41	15.92	459.1287	2-methylthio-N6-threonylcarbamoyladenosine	−1.3
42[a]	16.7	298.0986	5′-deoxy-5′-(methylthio)adenosine	5
43[c]	22.38	525.1957	hydroxywybutosine	3.2

[a]Manually extracted ion pairs for different neutral loss type. [b]Verified by nucleoside standards. [c]Reported for the first time.

molecular weights of 10000 and 750000 were grafted onto the Fe_3O_4@SiO_2. The results of the adenosine extraction showed that the adsorption capacity of Fe_3O_4@SiO_2@PEI(750T)-FPBA (1.34 ± 0.024 mg/g) is larger than that of Fe_3O_4@SiO_2@PEI(10T)-FPBA (0.94 ± 0.002 mg/g). The attractive adsorption capacity of Fe_3O_4@SiO_2@PEI(750T)-FPBA is 6−7-fold higher than that of analogous materials in previous reports,[22,25] and the adsorption capacity of Fe_3O_4@SiO_2@PEI(750T)-FPBA is also higher than that of commercial BAG (0.87 ± 0.04 mg/g).

To investigate the specificity of Fe_3O_4@SiO_2@PEI(750T)-FPBA, the 1,2-cis-diol ribonucleosides m1A and G were chosen as targets while DA and Gm were used as noncis-diol interferences. As shown in Figure 3 (panels a−c), only m1A and G can be enriched by our nanoparticles even if the molar ratio of interferences to targets increased from 1:1 to 100:1. What is even more revealing is that the signal intensities of m_1A and G after enrichment were nearly stable when the amount of the interferences was raised. To further verify the specificity of our nanoparticles toward 1,2-cis-diol compounds, the interferences from the 1,3-cis-diol compounds pG and iiG were investigated. When the molar ratio of the interferences to the targets was increased from 100:1 to 1000:1, the signal intensities of m_1A and G were so weak before enrichment that they were difficult to distinguish from the background, as shown in Figure 3 (panels d and e). Particularly, m_1A greatly was interfered because its retention time was close to that of iiG. After enrichment by the nanoparticles, the 1,3-cis-diol compounds (pG and iiG) were excluded, and only the 1,2-cis-diol compounds (m_1A and G) were extracted. These results

dx.doi.org/10.1021/ac402979w | Anal. Chem. 2013, 85, 11585−11592

prove that the nanoparticles have a very high specificity toward ribose conjugates.

The recovery of the 12 nucleosides from urine using the nanoparticles was measured, and their added concentration was similar to that in the urine sample.[35] The ideal relative recoveries (80−120%) with acceptable RSD values (<20%) were achieved for most of the nucleosides, except for Pseu and C, as shown in Figure S6 of the Supporting Information. The relatively low recoveries of Pseu and C can be attributed to their super hydrophilic properties, which reduce their affinities toward boronate.[20] Therefore, Fe_3O_4@SiO_2@PEI-FPBA can be applied to enrich the ribose conjugates for subsequent qualitative and quantitative analyses.

Enrichment and Identification of Ribose Conjugates from Urine. By virtue of large adsorption capacity and excellent selectivity, Fe_3O_4@SiO_2@PEI-FPBA was applied to enrich the ribose conjugates, including modified nucleosides and other ribosylated metabolites, from urine. Three technical replicates were carried out, and the treated urine samples were analyzed by LC coupled with high-resolution MS.

Neutral loss of the ribose moiety (132 u) has been widely used for the identification of urinary ribonucleosides.[13,14] With the help of in-house developed neutral loss software, a total of 60 ion-pairs with an $S/N > 3$ were extracted from urine after enrichment, as listed in Table S3 of the Supporting Information. Among them, 43 ion pairs were identified to be ribose conjugates with mass errors of within 20 ppm, as listed in Table 1. In these identified compounds, many modified nucleosides and ribosylated metabolites in low abundances were captured, such as 5-methoxycarbonylmethyl-2-thiouridine, 1-ribosyl-*N*-*ω*-valerylhistamine, 1-ribosyl-3-carbamoylpyridinium, 1-ribosyl-4-carboxamido-5-aminoimidazole, and *S*-adenosylhomocysteine. These metabolites are from RNA, nicotinate/nicotinamide, histidine, purine biosynthesis or methionine/polyamin cycle metabolism.[36,37] As shown in Figure 4, the MS signals of these ribosylated metabolites were greatly enhanced after enrichment, and some of them were even newly observed, such as peaks 35, 37, and 38. To the best of our knowledge, nine of the modified nucleosides identified from the urine samples have never been reported in the previous literature.[2,36−39] Although 17 of the other compounds are unknown, they can still be deduced to be ribose conjugates by the neutral loss of the ribose moiety (132 u). An ion pair such as 293.1131/161.0691 at a t_R of 3.85 min has also been reported before,[40] whose IDA information (Figure S7 of the Supporting Information) directly confirms the loss of 161.0691 from 293.1131.

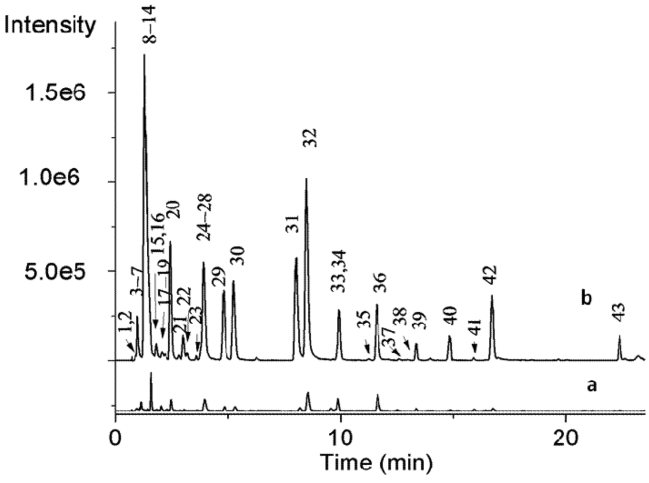

Figure 4. Extracted ion chromatograms of the urine analyzed directly (a) and after enrichment by Fe_3O_4@SiO_2@PEI (750T)-FPBA nanoparticles (b). Peaks marked with 1−43 correspond to those listed in Table 1

In this work, 39 1,2-cis-diol nucleosides were enriched and identified in a single analysis, which is better than in previous reports.[36,37,39,40] In comparison with the commercial adsorbents of BAG, 43 ion pairs of ribose conjugates, including 36 identified compounds and 7 unknown compounds, were also captured simultaneously by BAG among the 60 ion pairs extracted by Fe_3O_4@SiO_2@PEI(750T)-FPBA as listed in Table S3 of the Supporting Information (see footnote *a*). At the same time, Fe_3O_4@SiO_2@PEI(750T)-FPBA has a better performance than BAG from the rest of the 17 ion pairs of ribose conjugates enriched only by our material.

CONCLUSIONS

In summary, a novel type of magnetic nanoparticle named Fe_3O_4@SiO_2@PEI-FPBA was synthesized for capturing modified nucleosides and ribosylated metabolites. Benefiting from engraftment of PEI polymers onto the surface, Fe_3O_4@SiO_2@PEI-FPBA possessed the following advantages. (i) Numerous primary amines on the chains of PEI can bind a large number of 4-FPBA, which greatly improved the adsorption capacity. (ii) Secondary amines and tertiary amines on the chains of PEI strengthened the hydrophilic property of the materials, which would favor a decrease in the nonspecific adsorption. (iii) PEI chains as space arms can reduce the steric hindrance and flexibly capture the targets from complex matrices. After enrichment by the nanoparticles, 60 ion pairs of ribose conjugates were detected from real urine, and 43 were identified to be nucleosides or ribosylated metabolites. Nine modified nucleosides in low abundances were observed for the first time from urine. Fe_3O_4@SiO_2@PEI-FPBA exhibited powerful adsorption capability and good selectivity as well as being complementary to commercialized boronate affinity gel. Therefore, we expect the promising application of this novel material in the area of metabonomics to discover new cancer-related biomarkers.

ASSOCIATED CONTENT

Supporting Information

Supplementary tables and figures, such as the MRM parameters of the nucleoside standards, the chemical compositions of the nanoparticles, FT-IR spectra, the ion pairs with a neutral loss of m/z 132.0423 from the urine after enriched by Fe_3O_4@SiO_2@PEI(750T)-FPBA, the optimization of the adsorption and desorption conditions of Fe_3O_4@SiO_2@PEI-FPBA, the relative recoveries of nucleosides from the urine by Fe_3O_4@SiO_2@PEI(750T)-FPBA, and the IDA information of the unknown compounds are listed. This material is available free of charge via the Internet at http://pubs.acs.org.

AUTHOR INFORMATION

Corresponding Authors

*E-mail: shixianzhe@dicp.ac.cn.
*E-mail: xugw@dicp.ac.cn.

Notes

The authors declare no competing financial interest.

■ ACKNOWLEDGMENTS

This study was supported by the National Basic Research Program (Grants 2012CB720801 and 2012CB518303) from the State Ministry of Science and Technology of China, the foundation (Grants 21175132 and 21275141), and the creative research group project (Grant 21021004) from the National Natural Science Foundation of China.

■ REFERENCES

(1) Gustilo, E. M.; Franck, A. P. F.; Agris, P. F. *Curr. Opin. Microbiol.* **2008**, *11*, 134−140.
(2) Schram, K. H. *Mass Spectrom. Rev.* **1998**, *17*, 131−251.
(3) Nakano, K.; Nakao, T.; Schram, K. H.; Hammargren, W. M.; Mcclure, T. D.; Katz, M.; Petersen, E. *Clin. Chim. Acta* **1993**, *218*, 169−183.
(4) Itoh, K.; Konno, T.; Sasaki, T.; Ishiwata, S.; Ishida, N.; Misugaki, M. *Clin. Chim. Acta* **1992**, *206*, 181−189.
(5) Hsu, W. Y.; Chen, W. T. L.; Lin, W. D.; Tsai, F. J.; Tsai, Y.; Lin, C. T.; Lo, W. Y.; Jeng, L. B.; Lai, C. C. *Clin. Chim. Acta* **2009**, *402*, 31−37.
(6) Frickenschmidt, A.; Frohlich, H.; Bullinger, D.; Zell, A.; Laufer, S.; Gleiter, C. H.; Liebich, H.; Kammerer, B. *Biomarkers* **2008**, *13*, 435−449.
(7) Jiang, Y. Q.; Ma, Y. F. *Anal. Chem.* **2009**, *81*, 6474−6480.
(8) Fromentin, E.; Gavegnano, C.; Obikhod, A.; Schinazi, R. F. *Anal. Chem.* **2010**, *82*, 1982−1989.
(9) Yang, J.; Xu, G. W.; Kong, H. W.; Zheng, W. F.; Pang, T.; Yang, Q. *J. Chromatogr., B* **2002**, *78*, 27−33.
(10) Struck, W.; Siluk, D.; Yumba-Mpanga, A.; Markuszewski, M.; Kaliszan, R.; Markuszewski, M. J. *J. Chromatogr., A* **2013**, *1283*, 122−131.
(11) Dudley, E.; Lemiere, F.; Van Dongen, W.; Langridge, J. I.; El-Sharkawi, S.; Games, D. E.; Esmans, E. L.; Newton, R. P. *Rapid Commun. Mass Spectrom.* **2001**, *15*, 1701−1707.
(12) Tuytten, R.; Lemiere, F.; Esmans, E. L.; Herrebout, W. A.; van der Veken, B. J.; Maes, B. U. W.; Witters, E.; Newton, R. P.; Dudley, E. *Anal. Chem.* **2007**, *79*, 6662−6669.
(13) Tuytten, R.; Lemiere, F.; Van Dongen, W.; Witters, E.; Esmans, E. L.; Newton, R. P.; Dudley, E. *Anal. Chem.* **2008**, *80*, 1263−1271.
(14) Teichert, F.; Winkler, S.; Keun, H. C.; Steward, W. P.; Gescher, A. J.; Farmer, P. B.; Singh, R. *Rapid Commun. Mass Spectrom.* **2011**, *25*, 2071−2082.
(15) Hsu, W. Y.; Lin, W. D.; Tsai, Y. H.; Lin, C. T.; Wang, H. C.; Jeng, L. B.; Lee, C. C.; Lin, Y. C.; Lai, C. C.; Tsai, F. J. *Clin. Chim. Acta* **2011**, *412*, 1861−1866.
(16) Whiting, M. J. *Ann. Clin. Biochem.* **2009**, *46*, 129−136.
(17) James, T. D.; Sandanayake, K. R. A. S.; Shinkai, S. *Angew. Chem., Int. Ed.* **1996**, *35*, 1910−1922.
(18) Bullinger, D.; Neubauer, H.; Fehm, T.; Laufer, S.; Gleiter, C. H.; Kammerer, B. *BMC Biochem.* **2007**, *8*, 25.
(19) Ren, L. B.; Liu, Y. C.; Dong, M. M.; Liu, Z. *J. Chromatogr., A* **2009**, *1216*, 8421−8425.
(20) Liu, Y. C.; Ren, L. B.; Liu, Z. *Chem. Commun.* **2011**, *47*, 5067−5069.
(21) Xu, Y. W.; Wu, Z. X.; Zhang, L. J.; Lu, H. J.; Yang, P. Y.; Webley, P. A.; Zhao, D. Y. *Anal. Chem.* **2009**, *81*, 503−508.
(22) Wang, S. T.; Chen, D.; Ding, J.; Yuan, B. F.; Feng, Y. Q. *Chem.—Eur. J.* **2013**, *19*, 606−612.
(23) Xu, G.; Zhang, W.; Wei, L.; Lu, H.; Yang, P. *Analyst* **2013**, *138*, 1876−1885.
(24) Zhang, X. H.; He, X. W.; Chen, L. X.; Zhang, Y. K. *J. Mater. Chem.* **2012**, *22*, 16520−16526.
(25) Dou, P.; Liang, L.; He, J. G.; Liu, Z.; Chen, H. Y. *J. Chromatogr., A* **2009**, *1216*, 7558−7563.
(26) Liang, L. A.; Liu, Z. *Chem. Commun.* **2011**, *47*, 2255−2257.
(27) Liu, S. S.; Chen, H. M.; Lu, X. H.; Deng, C. H.; Zhang, X. M.; Yang, P. Y. *Angew. Chem., Int. Ed.* **2010**, *49*, 7557−7561.
(28) Zhao, L.; Qin, H.; Hu, Z.; Zhang, Y.; Wu, R. a.; Zou, H. *Chem. Sci.* **2012**, *3*, 2828−2838.
(29) Wang, Y.; Teng, X. W.; Wang, J. S.; Yang, H. *Nano Lett.* **2003**, *3*, 789−793.
(30) Tian, Y.; Yu, B. B.; Li, X.; Li, K. *J. Mater. Chem.* **2011**, *21*, 2476−2481.
(31) Yi, D. K.; Selvan, S. T.; Lee, S. S.; Papaefthymiou, G. C.; Kundaliya, D.; Ying, J. Y. *J. Am. Chem. Soc.* **2005**, *127*, 4990−4991.
(32) Liebich, H. M.; DiStefano, C.; Wixforth, A.; Schmid, H. R. *J. Chromatogr., A* **1997**, *763*, 193−197.
(33) Liu, L. T.; Zhang, Y.; Zhang, L.; Yan, G. Q.; Yao, J.; Yang, P. Y.; Lu, H. J. *Anal. Chim. Acta* **2012**, *753*, 64−72.
(34) Yan, J.; Fang, H.; Wang, B. H. *Med. Res. Rev.* **2005**, *25*, 490−520.
(35) Li, F. L.; Zhao, X. J.; Wang, W. Z.; Xu, G. W. *Anal. Chim. Acta* **2006**, *580*, 181−187.
(36) Henneges, C.; Bullinger, D.; Fux, R.; Friese, N.; Seeger, H.; Neubauer, H.; Laufer, S.; Gleiter, C. H.; Schwab, M.; Zell, A.; Kammerer, B. *BMC Cancer* **2009**, *9*, 104.
(37) Bullinger, D.; Fux, R.; Nicholson, G.; Plontke, S.; Belka, C.; Laufer, S.; Gleiter, C. H.; Kammerer, B. *J. Am. Soc. Mass. Spectrom.* **2008**, *19*, 1500−1513.
(38) Cantara, W. A.; Crain, P. F.; Rozenski, J.; McCloskey, J. A.; Harris, K. A.; Zhang, X. N.; Vendeix, F. A. P.; Fabris, D.; Agris, P. F. *Nucleic Acids Res.* **2011**, *39*, D195−201.
(39) Kammerer, B.; Frickenschmidt, A.; Gleiter, C. H.; Laufer, S.; Liebich, H. *J. Am. Soc. Mass. Spectrom.* **2005**, *16*, 940−947.
(40) Kammerer, B.; Frickenschmidt, A.; Muller, C. E.; Laufer, S.; Gleiter, C. H.; Liebich, H. *Anal. Bioanal. Chem.* **2005**, *382*, 1017−1026.